*Now with Acoustics Division, Naval Research Laboratory, Washington, D. C.
[1]G. Morpurgo, Phys. Rev. 110, 721 (1958).
[2]D. Kurath, Phys. Rev. 130, 1525 (1963).
[3]L. W. Fagg, W. L. Bendel, R. A. Tobin, and H. F. Kaiser, Phys. Rev. 171, 1250 (1968).
[4]L. W. Fagg, W. L. Bendel, E. C. Jones, Jr., and S. Numrich, Phys. Rev. 187, 1378 (1969).
[5]W. L. Bendel, L. W. Fagg, E. C. Jones, Jr., H. F. Kaiser, and S. Numrich, Bull. Am. Phys. Soc. 13, 1373 (1968).
[6]M. Rosen, R. Raphael, and H. Überall, Phys. Rev. 163, 927 (1967).
[7]B. T. Chertok, W. T. K. Johnson, and D. Sarkar, *"Table of Coulomb Distortation Corrections to Inelastic Electron Scattering Cross Sections for Magnetic-Dipole & -Quadrupole Transitions"* (The American University, Department of Physics, Washington, D. C., 1970).
[8]D. Drechsel, Nucl. Phys. A113, 665 (1968).
[9]W. L. Bendel, L. W. Fagg, R. A. Tobin, and H. F. Kaiser, Phys. Rev. 173, 1103 (1968).
[10]C. Toepffer and D. Drechsel, Z. Physik 210, 423 (1968).
[11]L. W. Fagg, E. C. Jones, Jr., and W. L. Bendel, Nucl. Instr. Methods 77, 136 (1970).
[12]L. C. Maximon, Rev. Mod. Phys. 41, 193 (1969). We employ the equation for inelastic scattering at the bottom of p. 199, but in the part-exponential form of the equation on p. 201.
[13]E. C. Jones, Jr., *et al.*, to be published.
[14]R. C. Ritter, J. T. Parson, and D. L. Bernard, Phys. Letters 28B, 588 (1969).
[15]B. T. Lawergren, A. T. G. Ferguson, and G. C. Morrison, Nucl. Phys. A108, 325 (1968).
[16]J. D. Pearson and R. H. Spear, Nucl. Phys. 54, 434 (1964).
[17]R. M. Polichar, J. E. Steigerwalt, J. W. Sunier, and J. R. Richardson, Phys. Rev. 163, 1084 (1967).
[18]J. W. Sunier, A. J. Armini, R. M. Polichar, and J. R. Richardson, Phys. Rev. 163, 1091 (1967).
[19]C. M. Lederer, J. M. Hollander, and I. Perlman, *Table of Isotopes* (John Wiley & Sons, Inc., New York, 1967), 6th ed.
[20]P. A. Quin and S. E. Vigdor, Bull. Am. Phys. Soc. 15, 1686 (1970); P. A. Quin, G. A. Bissinger, and P. R. Chagnon, Nucl. Phys. A115, 495 (1970).
[21]L. W. Fagg, W. L. Bendel, L. Cohen, E. C. Jones, Jr., and H. Überall, Bull. Am. Phys. Soc. 15, 1665 (1970).
[22]S. G. Nilsson, Kgl. Danske Videnskab. Selskab, Mat.-Fys. Medd. 29, No. 16 (1955).
[23]G. R. Bishop, Nucl. Phys. 14, 376 (1959).
[24]Y. Akiyama, A. Arima, and T. Sebe, Nucl. Phys. A138, 273 (1969).

PHYSICAL REVIEW C VOLUME 3, NUMBER 5 MAY 1971

Quasielastic Electron Scattering from ^{3}He and ^{3}H†

D. R. Lehman*
Center for Radiation Research, National Bureau of Standards, Washington, D. C. 20234
(Received 9 December 1970)

Quasielastic electron scattering from ^{3}He and ^{3}H is investigated with a model in which the two-nucleon interaction is described by a separable potential. Cross sections are given in the impulse approximation for the ejected proton and scattered electron detected in coincidence, and for detection of only the scattered electron. Both two- and three-body breakup of ^{3}He and ^{3}H are considered, with final-state interactions between the spectator nucleons included in three-body breakup. Good agreement is obtained with all the electrodisintegration data, except the ^{3}He coincidence data, for wave functions derived from separable potentials which reproduce the s-wave two-nucleon phase shifts at low and medium energies. Rescattering corrections between the spectator particles are found to be important in calculating three-body disintegration. The need for more refined and reliable coincidence data is reaffirmed.

I. INTRODUCTION

Electron scattering is a powerful tool to probe the structure of the trinucleons, ^{3}He and ^{3}H, and to obtain information about nucleon-nucleon interactions. The electric charge and magnetic form factors of ^{3}He and ^{3}H, which provide information about the three-nucleon ground state, can be measured by elastic electron scattering. Electrons scattered inelastically from the trinucleons also are sensitive to the ground-state wave function, but such experiments also involve the three-nucleon continuum states. A great amount of work has been done both experimentally and theoretically on elastic electron scattering,[1,2] but the work on inelastic electron scattering from ^{3}He and ^{3}H has been more limited.

^{3}He and ^{3}H inelastic electron scattering experiments have involved both low and high nuclear excitation energies, but no pion production. The most recent experiments have been concerned with the threshold region.[3] Frosch *et al.* have searched for excited states of ^{3}He by measuring inelastic spectra up to 17-MeV excitation energy.

The $M1$ continuum in ^{3}He has been studied by Chertok *et al.* with 180° scattering. Prior to these experiments, effort was concentrated on the quasielastic region.[4] The first was the coincidence experiment of Johansson. He measured electron-proton coincidences for both ^{3}He and ^{3}H. Following these measurements, Collard *et al.* and, later, Hughes *et al.* measured the inelastic cross sections throughout the quasielastic region, again for both ^{3}He and ^{3}H.[5] Until recently, theoretical effort[6] has centered on the Johansson and Collard *et al.* experiments.

The coincidence experiments of Johansson measured the cross sections for

$$\text{(A)}\quad e+{}^3\text{He}\to e'+p+\text{D},$$

$$\text{(B)}\quad \to e'+p+n+p,$$

$$\text{(C)}\quad e+{}^3\text{H}\to e'+p+n+n,$$

and theoretical effort has been devoted mainly to reaction (A). Griffy and Oakes[6] analyzed reaction (A) in the impulse approximation, keeping only those terms corresponding to scattering from the ejected proton. The interaction between the proton and deuteron was neglected, which should be a valid approximation at the quasielastic peak. The coincidence cross section was then shown to depend on the momentum distribution in the bound state of the ejected proton. As a result, the theoretical analysis distinguished markedly among various radial forms of the three-body ground state. They extended their work to reactions (B) and (C) by means of dispersion theory and thus eliminated the need for detailed knowledge of wave functions (see Appendix C). Griffy and Oakes calculated the cross sections on the basis that the proton-pole term dominates and the relative energy of the spectator nucleons is zero. This model reproduces the shape of the coincidence data, but does not predict the amplitude, since the constant vertex parameters are undetermined. If the vertex parameters are chosen on the basis of the coincidence data, then the predicted inelastic cross sections are 30 to 70% higher than the experimental points. A reanalysis of the coincidence data by Gibson and West[6] resulted in qualitative agreement, but is limited because of the ambiguities in interpreting the experimental data and the lack of an accurate calculation of the three-body coincidence cross section.[7] Thus these circumstances, along with the availability of the Hughes *et al.* data,[4] indicate the importance of an accurate three-body coincidence calculation and of a calculation of the inelastic cross sections without use of the coincidence data.

The objective of this paper is to describe a theoretical analysis for the reactions

$$e+{}^3\text{He}\ ({}^3\text{H})\to e'+\text{D}+p\ (n), \tag{1}$$

$$\to e'+n+p+p\ (n), \tag{2}$$

based solely on an assumed form of the two-nucleon interaction, thus eliminating the need to fit parameters to three-body data.[8] In Secs. II–IV we describe the model employed and derive the coincidence and inelastic cross sections. Section V contains a discussion of the separable nucleon-nucleon interaction which is used, along with a description of the resulting ground-state wave functions. The results and conclusions are given in Secs. VI and VII, respectively.

II. MODEL

The model we use to study quasielastic electron scattering from ^{3}He and ^{3}H is similar to that used by Griffy and Oakes, and later by Gibson and West.[6] The experiments of interest involve electrons with energies of hundreds of MeV's, indicating that the extreme relativistic limit is valid and that the incident and final electrons can be treated in the Born approximation. The high electron energy also implies that the electron-nucleus interaction can be handled in the impulse approximation. Consequently, we retain only those contributions corresponding to the electron interacting with the ejected nucleon. In both the two-body and three-body final states, we neglect interactions between the ejected nucleon and the spectator pair, but include final-state interactions between the spectator particles. Graphically, these considerations lead us to diagrams like those in Fig. 1.

The graphs of Fig. 1 display the approximations delineated in the previous paragraph. The electron-photon vertex is handled by standard techniques. The vertices of major concern are the nuclear ones. Figure 1(c) indicates, as an example, how we decompose the p-D-^{3}He vertex. Graph (1) corresponds to the case where the ejected nucleon interacts with the electron, whereas graph (2) depicts the situation where the ejected particle is not the one which interacted with the electron. We keep only contributions like graph (1), since contributions from graph (2) can be shown to be of minor importance at these energies (see Appendix C). The electron-nucleon interaction is treated by use of the McVoy–Van Hove interaction,[9] and the nuclear states are described by nonrelativistic wave functions. All intermediate nuclear states are taken to be on the mass shell, and we do not consider meson-exchange effects.

The effective Hamiltonian for the interaction between an electron and a nucleon of mass M is[9]

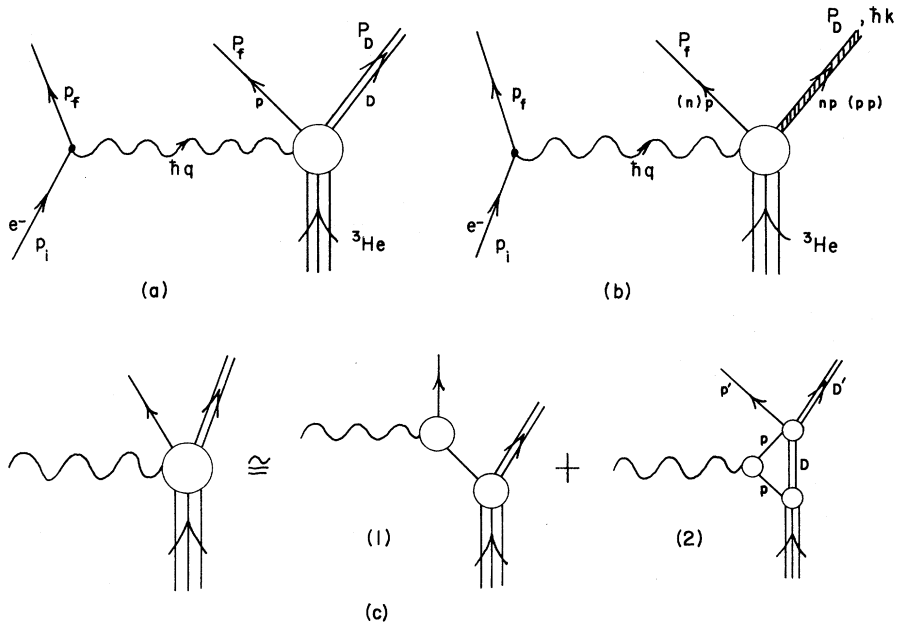

FIG. 1. Typical graphs in electrodisintegration of ^{3}He. (a) and (b) show the one-photon-exchange two- and three-body breakup of ^{3}He. (c) shows the decomposition of the p-D-^{3}He nuclear vertex into the proton pole (1) and a correction to the proton pole (2). All intermediate states are on the mass shell.

$$H_j'^N = -\frac{4\pi e^2}{q^2}\left\langle u_f \left| F_{1N}(q^2)\, e^{-i\vec{q}\cdot\vec{x}_j} - \frac{1}{2Mc}F_{1N}(q^2)\,(\vec{\mathrm{P}}_j\cdot\vec{\alpha}\, e^{-i\vec{q}\cdot\vec{x}_j} + e^{-i\vec{q}\cdot\vec{x}_j}\vec{\alpha}\cdot\vec{\mathrm{P}}_j)\right.\right.$$
$$\left.\left. - \frac{\hbar}{2Mc}[F_{1N}(q^2)+\kappa_N F_{2N}(q^2)]\, i\vec{\sigma}_j\cdot(\vec{q}\times\vec{\alpha})e^{-i\vec{q}\cdot\vec{x}_j} + \frac{\hbar^2 q^2}{8M^2c^2}[F_{1N}(q^2)+2\kappa_N F_{2N}(q^2)]e^{-i\vec{q}\cdot\vec{x}_j}\right| u_i\right\rangle, \quad (3)$$

correct through order $\hbar^2q^2/M^2c^2$. The notation is as follows: $p_i=\hbar k_i$ and $p_f=\hbar k_f$ are the initial and final electron four momenta, $\hbar q=\hbar(k_i-k_f)$ is the four-momentum transfer at the vertex, the P's denote nucleon momenta, $\vec{\sigma}$ is the nucleon spin operator, and the subscript j denotes the jth nucleon. F_{1N} and F_{2N} are the Dirac and Pauli nucleon form factors, and κ_N is the static anomalous magnetic moment in nuclear magnetons. $\vec{\alpha}$ is the electron's Dirac operator, which operates on the free-electron spinors $|u_i\rangle$ and $|u_f\rangle$. The range of validity of this form of the electron-nucleon interaction is estimated by McVoy and Van Hove to be $q^2 \lesssim 6.2$ fm^{-2}, sufficient for the experiments of interest.

Equation (3) describes the electron-nucleon interaction for an unbound nucleon. To handle the nuclear case, we make the usual assumption that the nucleons in a nucleus do not differ greatly from free nucleons. This permits use of the free-nucleon form factors. Then, since the operators for distinct nucleons commute, the electron-nucleus Hamiltonian is simply Eq. (3) summed over all nucleons present.[10]

The matrix element for the reactions under consideration can be written in the form

$$\langle f|H'|i\rangle = -\frac{4\pi e^2}{q^2}[\langle u_f|u_i\rangle Q - \langle u_f|\vec{\alpha}|u_i\rangle\cdot\vec{\mathrm{J}}], \quad (4)$$

where

$$Q = F_{\mathrm{ch}}^{p}(q^2)\left(1+\frac{\hbar^2q^2}{8M^2c^2}\right)\left\langle f\left|\sum_{j=1}^{3} e^{-i\vec{q}\cdot\vec{x}_j}\tfrac{1}{2}(1+\tau_3)_j\right|i\right\rangle, \quad (5)$$

$$\vec{\mathrm{J}} = \left\langle f\left|\sum_{j=1}^{3}\left[\frac{F_{\mathrm{ch}}^{p}(q^2)}{2Mc}(\vec{\mathrm{P}}_j e^{-i\vec{q}\cdot\vec{x}_j} + e^{-i\vec{q}\cdot\vec{x}_j}\vec{\mathrm{P}}_j) + \frac{i\hbar}{2Mc}F_{\mathrm{mag}}^{p}(q^2)e^{-i\vec{q}\cdot\vec{x}_j}(\vec{\sigma}_j\times\vec{q})\right]\tfrac{1}{2}(1+\tau_3)_j\right.\right.$$
$$\left.\left. + \sum_{j=1}^{3}\left[\frac{i\hbar}{2Mc}F_{\mathrm{mag}}^{n}(q^2)e^{-i\vec{q}\cdot\vec{x}_j}(\vec{\sigma}_j\times\vec{q})\right]\tfrac{1}{2}(1-\tau_3)_j\right|i\right\rangle. \quad (6)$$

In the above expressions, we have used the nucleon charge and magnetic form factors, which are defined in terms of the Dirac and Pauli form factors as

$$F_{\rm ch}(q^2) = F_1(q^2) + \frac{\hbar^2 q^2}{4M^2c^2}\kappa F_2(q^2)\,, \tag{7}$$

$$F_{\rm mag}(q^2) = F_1(q^2) + \kappa F_2(q^2)\,. \tag{8}$$

We take the neutron charge form factor $F_{\rm ch}^n(q^2)$ to be zero,[11] and in computations use the three-pole fit to $F_{\rm ch}(q^2)$ and $F_{\rm mag}(q^2)$ given by Janssens *et al.*[12] The states $|i\rangle$ and $|f\rangle$ are the initial and final nuclear states, and the expressions $\frac{1}{2}(1\pm\tau_3)_j$ are the nucleon isospin projection operators.

The cross sections of interest are obtained in the usual manner. Their evaluation reduces essentially to consideration of the matrix elements Q and $\vec{J}$.

III. COINCIDENCE CROSS SECTIONS

The coincidence experiments measured the cross sections for reactions (A)–(C). Specifically, they are given as a function of proton angle when the electron energy and angle are kept fixed. The experimental conditions were such that the reaction can be considered coplanar, thus providing some simplification in the kinematics (see Appendix A for kinematical details). The incident and final electron energies are approximately 550 and 450 MeV, respectively, and the electron is detected at 50°. For these conditions, the laboratory energy of the detected proton is always ~100 MeV, and the relative energy of the spectator pair in three-body breakup is on the order of 10 MeV. The high proton energy justifies the impulse approximation, while the low relative energy of the spectator pair suggests that only s-wave interactions need to be considered for this pair.

In order to derive the coincidence cross sections explicitly, we must specify the initial- and final-state wave functions. The dominant component of the trinucleon ground state is fully symmetric under exchange of the spatial coordinates and we consider only this part. This function has the form

$$|i\rangle = (2)^{-1/2}\psi_0^s(123)[\chi'(123)\eta''(123) - \chi''(123)\eta'(123)]\,, \tag{9}$$

where $\psi_0^s(123)$ is the symmetric spatial part and the $\chi'(\eta')$ and $\chi''(\eta'')$ are the spin-$\frac{1}{2}$ (isospin-$\frac{1}{2}$) functions for three particles. The notation prime (double prime) signifies nucleons 2 and 3 coupled to spin or isospin 0 (1) and then coupled to nucleon 1 for total spin or isospin $\frac{1}{2}$. Of course, the final-state wave functions depend on the reaction. In evaluation of the matrix elements, we can write

$$|f\rangle = \sqrt{3}\,\varphi_S(1,23)\chi_{1/2}(1)\chi_S(23)\eta_{1/2}(1)\eta_T(23)\,, \tag{10}$$

where $\varphi_S(1,23)$ is the spatial function and S (T) is the spin (isospin) state of the 2-3 pair. The number $\sqrt{3}$ is introduced to take care of the effect of antisymmetrization. For two-body breakup, $\varphi_S(1,23)$ becomes $\varphi_1(1,23)$ and represents particle 1 free and 2-3 bound. Likewise, for three-body breakup, $\varphi_S(1,23)$ can be either $\varphi_1(1,23)$ or $\varphi_0(1,23)$, where again particle 1 is free but 2-3 are interacting in either a spin triplet or singlet s-wave scattering state.

Derivation of the coincidence cross sections is a straightforward, but lengthy task. We substitute Eq. (9) and the appropriate form of Eq. (10) into Eqs. (5) and (6), and perform the nuclear-spin sums as shown in Appendix B. The form of the coincidence cross sections is as follows:

(A) $e + {}^3\mathrm{He} \to e' + p + \mathrm{D}$,

$$\frac{d^3\sigma}{d\Omega_e d\Omega_p dE_f} = \tfrac{3}{2}\sigma_{\rm Mott}|M_1^B|^2\,; \tag{11}$$

(B) $e + {}^3\mathrm{He} \to e' + p + (np)$,

$$\frac{d^3\sigma}{d\Omega_e d\Omega_p dE_f} = \sigma_{\rm Mott}\int_0^{k_{\max}} d^3k\left[\tfrac{3}{2}|M_1^s(\vec{k})|^2 + \tfrac{1}{2}|M_0^s(\vec{k})|^2\right]; \tag{12}$$

(C) $e + {}^3\mathrm{H} \to e' + p + (nn)$,

$$\frac{d^3\sigma}{d\Omega_e d\Omega_p dE_f} = \sigma_{\rm Mott}\int_0^{k_{\max}} d^3k\,|M_0^s(\vec{k})|^2\,; \tag{13}$$

where

$$\sigma_{\rm Mott} = \tfrac{1}{4}\alpha^2\frac{\hbar^2c^2}{E_i^{\,2}}\frac{\cos^2\frac{1}{2}\theta}{\sin^4\frac{1}{2}\theta}\,. \tag{14}$$

In Eq. (11), $|M_1^B|^2$ is given by

$$|M_1^B|^2 = \frac{l_f M}{\hbar^2}\frac{1}{(2\pi)^3}\left(1 + \frac{M}{M_{\rm D}}\frac{\vec{l}_i\cdot\vec{l}_f}{l_f^{\,2}}\right)^{-1} F^B(\vec{l}_i,\vec{l}_f)\,, \tag{15}$$

where

$$F^B(\vec{l}_i,\vec{l}_f)=F_{\rm ch}^{p\,2}(q^2)\left[\left(1+\frac{\hbar^2q^2}{4M^2c^2}\right)|I_1+I_2|^2+\frac{1}{4M^2c^2}\tan^2\tfrac{1}{2}\theta\,|\vec{J}_1+\vec{J}_2|^2\right.$$
$$-\frac{1}{4Mc}\sec^2\tfrac{1}{2}\theta\{(\hat{k}_i+\hat{k}_f)\cdot[(\vec{J}_1+\vec{J}_2)^*(I_1+I_2)+(I_1+I_2)^*(\vec{J}_1+\vec{J}_2)]\}$$
$$\left.+\frac{1}{8M^2c^2}\sec^2\tfrac{1}{2}\theta[\hat{k}_f\cdot(\vec{J}_1+\vec{J}_2)^*\hat{k}_i\cdot(\vec{J}_1+\vec{J}_2)+\hat{k}_i\cdot(\vec{J}_1+\vec{J}_2)^*\hat{k}_f\cdot(\vec{J}_1+\vec{J}_2)]\right]$$
$$-(1+2\tan^2\tfrac{1}{2}\theta)\frac{\hbar^2q^2}{4M^2c^2}[F_{\rm mag}^{p\,2}(q^2)|I_1-I_2|^2+F_{\rm mag}^{n\,2}(q^2)|I_2|^2-\tfrac{2}{3}F_{\rm mag}^{p}(q^2)F_{\rm mag}^{n}(q^2)|I_2(I_1-I_2)|]. \quad (16)$$

We have used the notation $\vec{P}_f=\hbar\vec{l}_f$ and $\vec{P}_D=-\vec{P}_i=-\hbar\vec{l}_i$, where $\vec{P}_i$ represents the momentum of the ejected nucleon in the nucleus prior to ejection. $E_i\approx p_ic$, $E_f\approx p_fc$, and θ are the electron's initial energy, final energy, and scattering angle, respectively, while Ω is used to mean solid angle, α is the fine-structure constant, and $\vec{k}$ is the relative momentum of the spectator nucleons. The nuclear wave functions enter through the integrals I_1, I_2, $\vec{J}_1$, and $\vec{J}_2$. In the momentum representation, these integrals have the form:

$$I_1(\vec{l}_i)=(2\pi)^{3/2}\int d^3p\,\varphi_B^*(\vec{p})\psi_0^s(\vec{p},\vec{l}_i)\,, \quad (17)$$

$$I_2(\vec{l}_i,\vec{l}_f)=(2\pi)^{3/2}\int d^3p\,\varphi_B^*(\vec{p})\psi_0^s(\tfrac{1}{2}(\vec{p}+\vec{l}_f+\tfrac{1}{2}\vec{l}_i),\vec{p}-\vec{l}_f+\tfrac{1}{2}\vec{l}_i)\,, \quad (18)$$

$$\vec{J}_1(\vec{l}_i,\vec{l}_f)=(2\vec{l}_f-\vec{q})I_1(\vec{l}_i)\,, \quad (19)$$

$$\vec{J}_2(\vec{l}_i,\vec{l}_f)=(2\pi)^{3/2}2\int d^3p\,\varphi_B^*(\vec{p})\vec{p}\psi_0^s(\tfrac{1}{2}(\vec{p}+\vec{l}_f+\tfrac{1}{2}\vec{l}_i),\vec{p}-\vec{l}_f+\tfrac{1}{2}\vec{l}_i)-\vec{l}_fI_2(\vec{l}_i,\vec{l}_f)\,. \quad (20)$$

The expressions $|M_0^s(\vec{k})|^2$ and $|M_1^s(\vec{k})|^2$ differ in form only slightly from $|M_1^B|^2$. The same integrals as Eqs. (17)–(20) can be defined if $\varphi_B(\vec{p})$ is replaced by the appropriate scattering state $\varphi_k^{(-)}(\vec{p})$. However, $F^B(\vec{l}_i,\vec{l}_f)\to F^s(\vec{l}_i,\vec{l}_f,\vec{k})$, $M_D\to 2M$, and the magnetic-form-factor term in Eq. (16) changes. For the triplet part of reaction (B), $F^1(\vec{l}_i,\vec{l}_f,\vec{k})$ has the same form as Eq. (16); however, the singlet part has the factor $-\frac{2}{3}$ in front of the last term replaced by +2. Reaction (C) has only the magnetic-form-factor contribution

$$-(1+2\tan^2\tfrac{1}{2}\theta)\frac{\hbar^2q^2}{4M^2c^2}F_{\rm mag}^{p\,2}(q^2)|I_1|^2\,. \quad (21)$$

Now that we have the coincidence cross sections, it is interesting to note the correspondence of the terms with our graphs in the previous section. In Fig. 1(c), we have decomposed the basic vertex into two graphs: (1) pole dominance and (2) corrections to pole dominance. The pole-dominance graph corresponds to all contributions from the I_1 and $\vec{J}_1$ integrals, and the corrections to the I_2 and $\vec{J}_2$. It is the contributions from I_2 and $\vec{J}_2$ which can be neglected at these energies (see Appendix C), and from here on, I_2 and $\vec{J}_2$ will not be considered.

IV. INELASTIC CROSS SECTIONS

The inelastic experiments involve detection of only the electron at a given angle and energy. The experimental data involve incident electrons of approximately 250 and 450 MeV detected at 90 and 75°, respectively. As in the coincidence experiments, the data involve primarily the quasielastic region, for which our model is valid. However, the reaction can no longer be considered planar, and the distribution of energy among the nucleons is different. The spectator pair can now have a relative energy as great as 100 MeV. Naturally, this reduces the relative energy of the spectator-pair center of mass and the ejected nucleon, limiting our model to nuclear excitation energies greater than ~50 MeV. Below this excitation energy, we would expect three-body rescattering corrections to be important.[13]

Once we have specified the final states, we can derive the inelastic cross sections. This is easily done if we classify the final states by isospin. For electrodisintegration of ^{3}He as an example, we have:

two-body ($I=\frac{1}{2}$),

$$|f\rangle=\sqrt{3}\,\varphi_B(1,23)\chi''(1,23)\eta'(1,23)\,; \quad (22)$$

three-body ($I=\frac{1}{2}$),

$$|f\rangle=\sqrt{3}\,\varphi_1(1,23)\chi''(1,23)\eta'(1,23)\,, \tag{23}$$

$$|f\rangle=\sqrt{3}\,\varphi_0(1,23)\chi'(1,23)\eta''(1,23)\,; \tag{24}$$

three-body ($I=\frac{3}{2}$),

$$|f\rangle=\sqrt{3}\,\varphi_0(1,23)\chi'(1,23)\eta^S(1,23)\,, \tag{25}$$

where $\eta^S(1,23)$ is the isospin-$\frac{3}{2}$ function with z projection $\frac{1}{2}$, and the remaining notation is as before. The inelastic cross section is obtained from the incoherent sum of the isospin amplitudes. When the I_2 and $\vec{J}_2$ integrals are neglected, we derive for ^{3}He

$$\frac{d^2\sigma}{dE_f d\Omega_e}=\sum_{R=1}^{4}\frac{d^2\sigma(R)}{dE_f d\Omega_e}\,, \tag{26}$$

where

$$\frac{d^2\sigma(R)}{dE_f d\Omega_e}=\int d\Omega_p\,\frac{d^3\sigma(R)}{dE_f d\Omega_e d\Omega_p}\,, \tag{27}$$

and R represents the following final states (subscripts 1 and 0 mean spin triplet and singlet, respectively):

$R=1$, $p+\mathrm{D}$;

$R=2$, $p+(np)_1$;

$R=3$, $p+(np)_0$;

$R=4$, $n+(pp)_0$;

and likewise for ^{3}H, only R represents the following final states:

$R=1$, $n+\mathrm{D}$;

$R=2$, $n+(np)_1$;

$R=3$, $n+(np)_0$;

$R=4$, $p+(nn)_0$.

Therefore, the ^{3}He-^{3}H inelastic cross sections are simply the sum of the given coincidence cross sections, with explicit forms given in Sec. IV, integrated over proton angles.[14]

V. WAVE FUNCTIONS

A separable-potential representation of the two-nucleon interaction permits an exact solution of the three-nucleon Schrödinger equation. We choose one of the simplest forms of the nonlocal, separable potential, that of Yamaguchi.[15] In the momentum representation, this potential has the form

$$\langle\vec{k}|\,V\,|\vec{k}'\rangle=-\frac{\lambda\hbar^2}{M}g^*(\vec{k})g(\vec{k}')\,, \tag{28}$$

and the form factor $g(\vec{k})$ is taken as

$$g(k)=(k^2+\beta^2)^{-1}\,. \tag{29}$$

The strength parameter λ and the range parameter β are determined by fitting low- to medium-energy (0 to ~100 MeV) properties of the two-nucleon system.

The spatial part of the three-nucleon ground state in the momentum representation is

$$\psi_0^s(\vec{k},\vec{p})=N[g_s(\vec{k},\vec{p})+g_s(\tfrac{3}{4}\vec{p}+\tfrac{1}{2}\vec{k},\vec{k}-\tfrac{1}{2}\vec{p}) +g_s(\tfrac{3}{4}\vec{p}-\tfrac{1}{2}\vec{k},-\vec{k}-\tfrac{1}{2}\vec{p})]\,, \tag{30}$$

where $\vec{k}$ is the relative momentum of a pair of the nucleons, and $\vec{p}$ is the relative momentum of the remaining nucleon relative to the center of mass of this pair. For a separable potential such as Eq. (28),

$$g_s(\vec{k},\vec{p})=2\lambda g(k)a(p)(k^2+\tfrac{3}{4}p^2+K^2)^{-1}\,, \tag{31}$$

with $-K^2/M$ equal to the three-nucleon binding energy. The sum $k^2+\frac{3}{4}p^2$ is invariant under permutations of particles. The function $g(k)$ appears in Eq. (28), and the spectator function $a(p)$ must be determined numerically from an integral equation. Along with the three-nucleon ground state, we also need the two-nucleon bound and scattering wave functions. They are given by

$$\varphi_B(k)=N_B g(k)(k^2+\gamma^2)^{-1}\,, \tag{32}$$

$$\varphi_{k_0}^{(-)}(\vec{k})=\delta^3(\vec{k}-\vec{k}_0)+\frac{f^*(k_0)g(k)}{2\pi^2 g(k_0)}\,\frac{1}{k^2-k_0^{\,2}+i\epsilon}\,, \tag{33}$$

$$f(k)=\left(\frac{1}{2\pi^2\lambda g^2(k)}+\frac{1}{2\beta g(k)}-\beta-ik\right)^{-1}\,, \tag{34}$$

with the two-nucleon binding energy equal to $-\gamma^2/M$. We use these expressions to evaluate the cross sections.[15,16]

Two sets of parameters are considered in our computations.[17] The first set is based on an effective-range analysis of the nucleon-nucleon scattering data, and we denote them by SK (Sitenko and Kharchenko).[18] The second set is that of Tabakin,[19] which provide a fit to the s-wave phase shifts at low and medium energies. We tabulate these parameters in Table I. From this table, we note that SK predict a three-nucleon binding energy of 12.55 MeV, whereas Tabakin's model 2 gives 9.33 MeV. The experimental binding energies of ^{3}He and ^{3}H are 7.71 and 8.48 MeV, respectively. The charge radii of these wave functions are 1.75 fm for Tabakin and 1.52 fm for SK when the proton charge radius is taken to be 0.80 fm, compared with the values obtained from elastic electron scattering $R_{\mathrm{ch}}(^3\mathrm{He})=1.87\pm0.05$ fm and $R_{\mathrm{ch}}(^3\mathrm{H})=1.70\pm0.05$ fm.[20] In Fig. 2, we give the charge form factors predicted by these wave func-

TABLE I. Parameters for separable interactions.

	SK	Tabakin
	Ground state	
β (fm^{-1})	1.450	1.150
λ (fm^{-3})	0.353	0.182
K (fm^{-1})	0.550	0.474
N (fm^2)	0.579	0.886
B.E. (MeV)	12.55	9.33
	Final-state triplet	
β_B (fm^{-1})	1.450	1.150
λ_B (fm^{-3})	0.415	0.220
γ (fm^{-1})	0.232	0.232
N_B (fm$^{-5/2}$)	0.402	0.266
	Final-state singlet	
β_0 (fm^{-1})	1.304	1.150
λ_0 (fm^{-3})	0.211	0.148

tions out to 8-fm^{-2} four-momentum transfer. As would be expected, the Tabakin ground state is superior and gives a good fit to the data[20] out to ~4 fm^{-2}.

The point should be made that only Tabakin's parameters are used for *both* the coincidence and inelastic cross-section calculations. The SK parameters are based on an effective-range analysis of the two-nucleon data and are not valid for relative energies exceeding ~10 MeV. Therefore the SK parameters are considered *only* in the coincidence calculations, since the relative energy of the spectator pair is always on the order of 10 MeV, in contrast to the inelastic data, where the relative energy of the spectator pair can be as great as ~100 MeV.

VI. RESULTS

The results for the coincidence cross sections are given in Figs. 3–5. Figures 3(a) and 3(b) compare the theoretical results with the two versions of the experimental data for the two-body breakup of ^{3}He. Figure 3(a) gives the experimental points as they were obtained by Johansson,[4] by subtracting the ^{3}H coincidence data (appropriately modified for threshold differences and divided by 2) from the total ^{3}He coincidences. Figure 3(b) shows the reanalysis of the data by Gibson and West.[6] Neither the Tabakin result, curve (A), nor the SK result, curve (B), agree with either set of data points. The Tabakin result is 45% below the data at the peak for the Johansson analysis and 30% below the peak for the Gibson-West analysis. The SK curve is 40% below the Tabakin curve at the peak. Contrasted with this poor agreement in the ^{3}He two-body case is the excellent agreement with experiment obtained for the Tabakin interaction in the ^{3}H case. This is especially interesting,

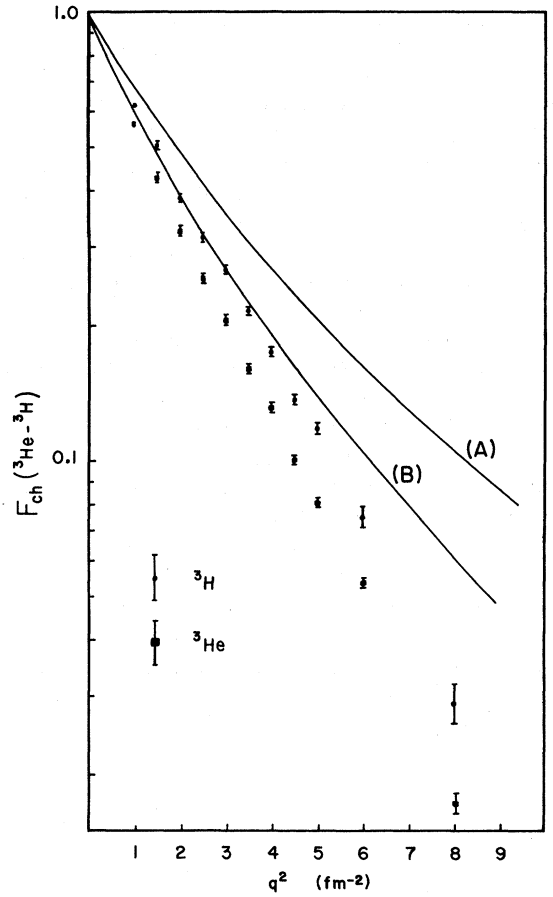

FIG. 2. Charge form factor. Curve (A) is the theoretical prediction with the Tabakin ground state and curve (B) with the SK ground state. The data are from Ref. 20.

since the ^{3}H coincidence data are three-body breakup. We show the results in Fig. 4(a). Though the Tabakin curve (A) agrees very well, the SK curve (B) does not. However in Fig. 4(b), agreement still is not attained when the Tabakin results for the two- and three-body breakup of ^{3}He are combined and compared with the total ^{3}He coincidence data. Yet in Fig. 5(a), our Tabakin theory implies that Johansson's method of subtracting the three-body coincidences from the total ^{3}He coincidences is reasonable. Finally, in Fig. 5(b), we see the importance of the singlet final-state interactions between the spectator nucleons for Tabakin's interaction. They enhance the result ~20% at the peak.

The results for the coincidence cross sections suggest that the Tabakin parameters give the best results. This is confirmed in the results for the inelastic cross sections. In Figs. 6(a) and 6(b) we give the theoretical curves for ^{3}H and ^{3}He superimposed on the Hughes *et al.* data[4] for initial electron energy equal to 398.4 MeV.[21] The agree-

ment with the experimental data is excellent over a range of final electron energies corresponding to excitation energies from ~40 to ~130 MeV.[22] In Figs. 7(a) and 7(b) we show similar results for initial electron energy equal to 248.8 MeV. The agreement with experiment is good for nuclear excitation energies from ~35 to ~90 MeV. No differences between the ^{3}H and ^{3}He results occur, in contrast to the coincidence case. Figures 8 and 9 display the two- and three-body contributions to the various cross sections. The three-body breakup is dominant in ^{3}H, whereas the two-body breakup is dominant in ^{3}He. We also note that the triplet three-body breakup is small for ^{3}He and negligible for ^{3}H. The role played by the final-state interactions is shown in Figs. 10 and 11. Final-state rescattering not only changes the amplitudes, but also changes the shape of the three-body contribution. Of course, final-state effects play a bigger role for ^{3}H than ^{3}He, but in both cases it makes the difference between good or poor agreement with experiment.

VII. DISCUSSION AND CONCLUSIONS

We have seen how a representation of the low-to-medium-energy two-nucleon s-wave interactions provides good agreement with the inelastic electron scattering data for ^{3}He and ^{3}H. Thus, within present experimental errors, quasielastic electron scattering requires only gross information about the two-nucleon interaction. However, singlet final-state rescattering between the spectator particles is an important effect and must be included. Therefore, the Griffy-Oakes[6] assumption that the relative energy of the spectator particles can be neglected is not valid.

We conclude that this simple model of electrodisintegration of ^{3}H and ^{3}He yields good results for the inelastic cross sections in the quasielas-

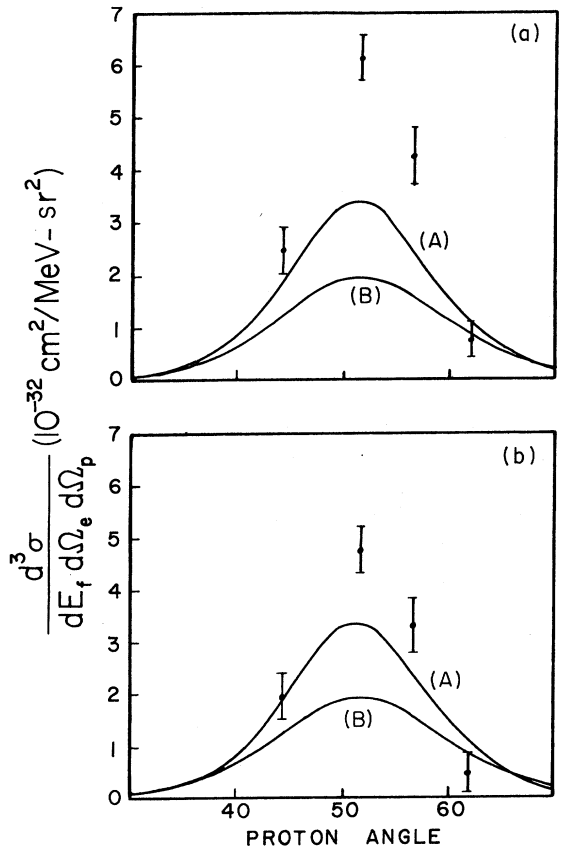

FIG. 3. Coincidence cross section for $e + {}^3\mathrm{He} \rightarrow e' + p + \mathrm{D}$. (a) The data as originally analyzed by Johansson, Ref. 4. (b) The reanalyzed data of Gibson and West, Ref. 6. Curve (A) is the theoretical result with Tabakin's parameters, and curve (B) with the SK parameters.

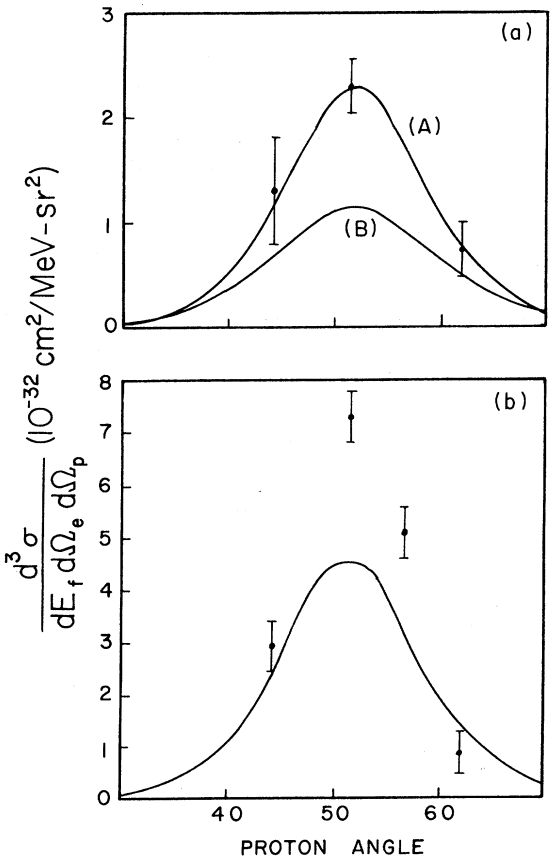

FIG. 4. (a) Coincidence cross section for electrodisintegration of ^{3}H. Curve (A) is from Tabakin's parameters, and curve (B) from the SK parameters. The data are from Johansson, Ref. 4. (b) Coincidence cross section for electrodisintegration of ^{3}He. The theoretical curve is obtained with Tabakin's parameters, and the data points are from Johansson, Ref. 4.

tic region, and indicates the limited validity of the coincidence data. Disagreement with the inelastic data is expected in the regions of low and high excitation energy. When the excitation energy is low, the three-particle aspects of the final-state interactions are important.[13] At high excitation energy, the cross section should be more sensitive to high-momentum components in the ground state. However, within these two extremes, the approximation of a spatially symmetric ground state corresponding to Tabakin's model 2 appears to be adequate within experimental errors. The disagreement of the model with the ^{3}He coincidence data seems to indicate that the experimental results of Johansson[4] could be incorrect by as much as 40% rather than his estimate of 20% in addition to statistics. Hopefully within the next few years, new coincidence measurements with higher reliability and more points can be made.

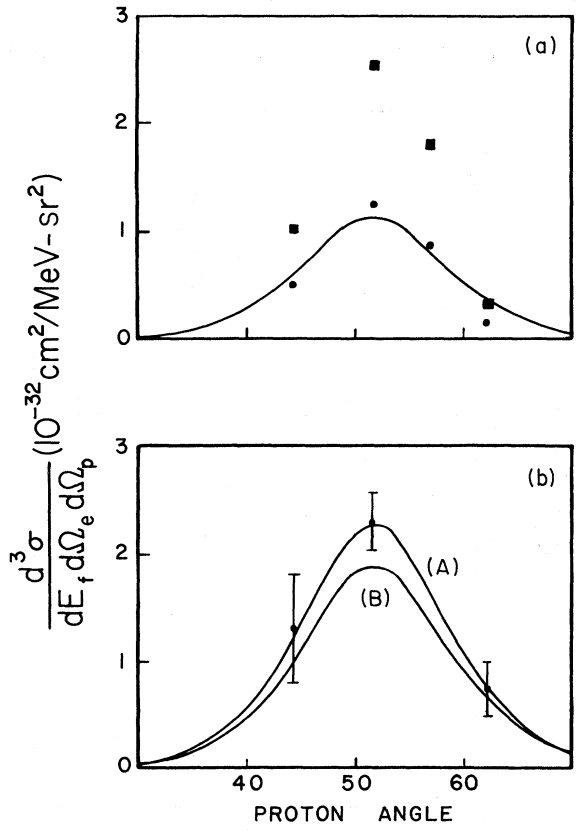

FIG. 5. (a) Coincidence cross section for $e+{}^3\mathrm{He}\rightarrow e'+p+(np)$. The theoretical curve is from Tabakin's parameters. The dots represent data points from Johansson, Ref. 4, and the blocks are from the reanalysis of Gibson-West, Ref. 6. (b) Coincidence cross section for electrodisintegration of ^{3}H. The theoretical curves show the Tabakin results with (A) and without (B) the singlet rescattering corrections for the spectator neutrons. The data points are from Johansson, Ref. 4.

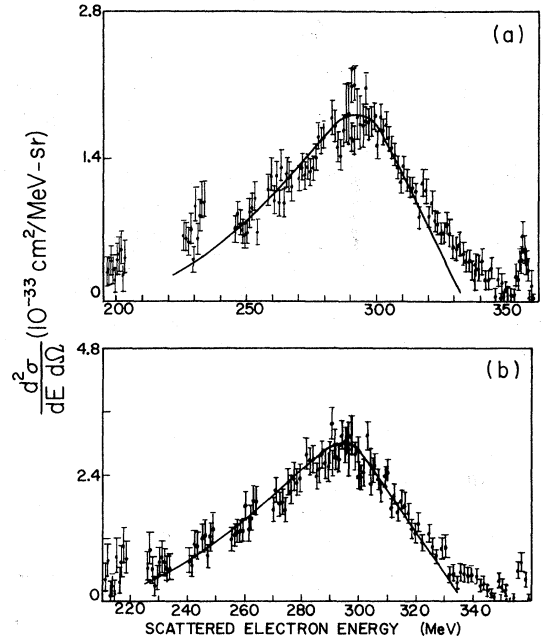

FIG. 6. Inelastic cross sections for electrodisintegration of ^{3}H, (a), and ^{3}He, (b), with $E_i=398.4$ MeV and $\theta=75°$. The solid curves are the theoretical results with Tabakin's parameters. The data are from Hughes, Yearian, and Hofstadter, Ref. 4.

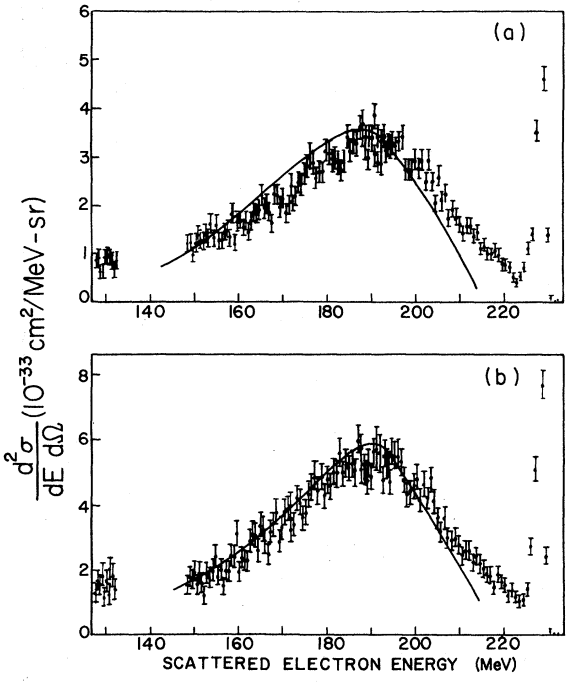

FIG. 7. Inelastic cross sections for electrodisintegration of ^{3}H, (a), and ^{3}He, (b), with $E_i=248.8$ MeV and $\theta=90°$. The solid curves are the theoretical results with Tabakin's parameters. The data are from Hughes, Yearian, and Hofstadter, Ref. 4.

ACKNOWLEDGMENTS

The author would like to thank Professor Francisco Prats for suggesting this problem and for valuable criticism throughout the course of the work. The author is also grateful to Dr. J. S. O'Connell for several discussions and to Dr. B. F. Gibson and Dr. E. B. Hughes for correspondence. He would like to thank Dr. E. Hayward for reading the manuscript. Computer time for this work was provided by the George Washington University Computer Center, and the author wishes to thank the computer center personnel for their assistance.

APPENDIX A. KINEMATICS

The kinematic equations are based on Fig. 12. We define a three-dimensional coordinate system with the incident- and final-electron momentum vectors. The incident momentum defines the z axis, and the final momentum defines the y-z plane. The nucleon momenta then lie out of the y-z plane, in general. Conservation of momentum leads to

$$p_i = p_f \cos\theta + P_f \cos\theta_p + P_D \cos\theta_D , \tag{A1}$$

$$0 = -p_f \sin\theta + P_f \sin\theta_p \sin\varphi_p + P_D \sin\theta_D \sin\varphi_D , \tag{A2}$$

$$0 = P_f \sin\theta_p \cos\varphi_p + P_D \sin\theta_D \cos\varphi_D . \tag{A3}$$

If $\varphi_p = 90°$ in Eqs. (A1)–(A3), then $\varphi_D = 90°$ and we have the equations applicable to the coincidence experiments. They are

$$p_i = p_f \cos\theta + P_f \cos\theta_p + P_D \cos\theta_D , \tag{A4}$$

$$0 = -p_f \sin\theta + P_f \sin\theta_p + P_D \sin\theta_D . \tag{A5}$$

The energy-conservation equations are the same for both experiments and can be written as

$$E_i = E_f + P_f^2/2M + P_D^2/2M_D + B_2 \tag{A6}$$

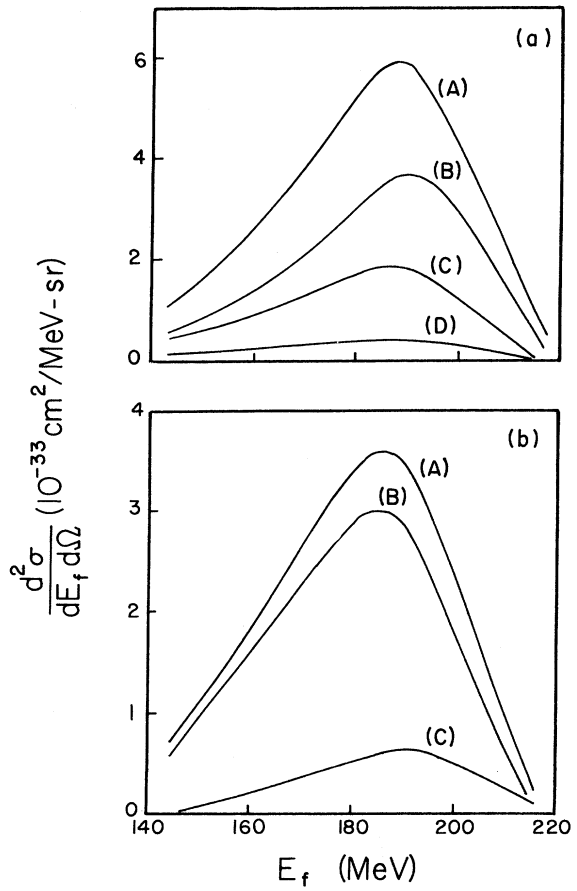

FIG. 8. Inelastic cross sections for $E_i = 398.4$ MeV and $\theta = 75°$. The curves are computed with Tabakin's parameters. (a) Decomposition of ^{3}He cross section (A) into the two-body (B), three-body singlet (C), and three-body triplet (D) contributions. (b) Decomposition of ^{3}H cross section (A) into the three-body (B) and two-body (C) contributions.

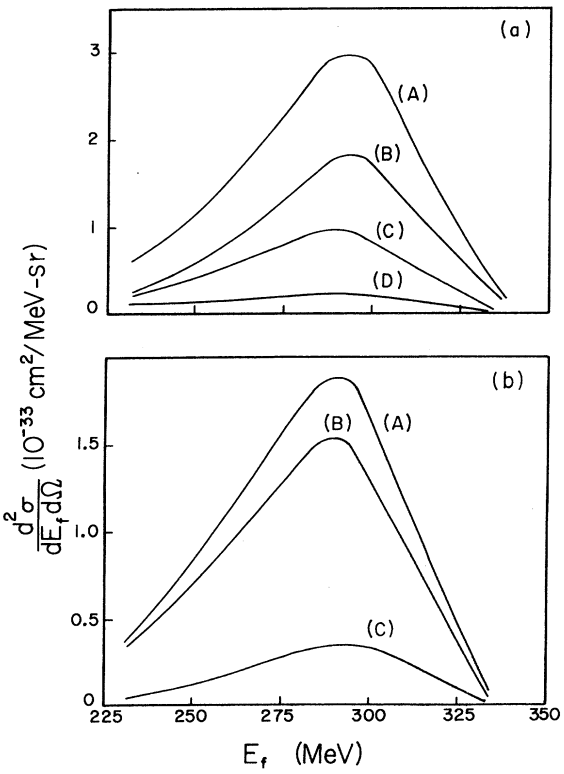

FIG. 9. Inelastic cross sections for $E_i = 248.8$ MeV and $\theta = 90°$. The curves are computed with Tabakin's parameters. (a) Decomposition of ^{3}He cross section (A) into the two-body (B), three-body singlet (C), and three-body triplet (D) contributions. (b) Decomposition of ^{3}H cross section (A) into the three-body (B) and two-body (C) contributions.

for two-body breakup, and

$$E_i = E_f + P_f^2/2M + P_D^2/4M + \hbar^2 k^2/M + B_3 \qquad \text{(A7)}$$

for three-body breakup. B_2 is the energy required to break the trinucleons into a deuteron plus nucleon, and B_3 is the trinucleon binding energy.

In the coincidence experiment, E_i, E_f, θ, θ_p, B_2, and B_3 are known, so only P_f, P_D, and θ_D are unknown in two-body breakup, but P_f, P_D, θ_D, and k are unknown in three-body breakup. Since there are three independent equations (A4)–(A6), all quantities are determined in two-body breakup. However, three-body breakup has one more unknown than independent equations – namely, k. We must, therefore, integrate over k in the cross sections from 0 to $k_{\max}$, where $k_{\max}$ is determined from the minimum proton energy in the experiment.

The inelastic cross sections are handled similarly, but $k_{\max}$ is now determined from the kinematics. Since we integrate over Ω_p, P_f can be expressed in terms of θ_p, φ_p, and k. In order that P_f remain real, it can be shown that

$$\gamma(k^2) \leq \tfrac{1}{12}(\alpha \cos\theta_p + \beta \sin\theta_p \sin\varphi_p)^2 \qquad \text{(A8)}$$

must be satisfied, where

$$\gamma(k^2) = 4(k^2 - E) + k_i^2 + k_f^2 - 2k_i k_f \cos\theta\,, \qquad \text{(A9)}$$

$$\alpha = 2(k_i - k_f \cos\theta)\,, \qquad \text{(A10)}$$

$$\beta = 2k_f \sin\theta\,, \qquad \text{(A11)}$$

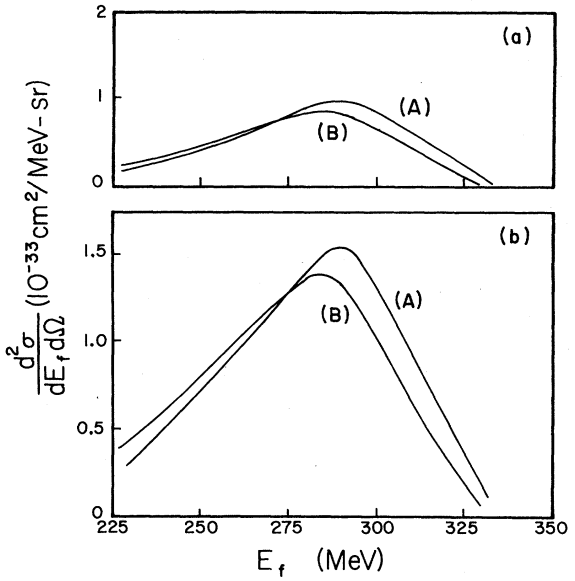

FIG. 10. Comparison of the three-body contribution to the inelastic cross sections, $E_i = 398.4$ MeV and $\theta = 75°$, with and without final-state interactions. Figures (a) and (b) give the results for ^{3}He and ^{3}H, respectively. Curves (A) are results with final-state rescattering between the spectator pair and curves (B) without. Tabakin's parameters are used in all cases.

$$E = M(E_i - E_f - B_3)/\hbar^2\,. \qquad \text{(A12)}$$

The equality in Eq. (A8) gives an equation to determine $k_{\max}$.

APPENDIX B. SPIN SUMS

The nuclear-spin sums are trivial except for the magnetic terms. As an example, a typical magnetic term of $\vec{J}^* \cdot \vec{J}$ for *two-body* breakup of ^{3}He is

$$F^n_{\rm mag}(q^2) F^p_{\rm mag}(q^2) I_1^* I_2 (1 + T_{12}) \chi_i'^{\dagger}(312) \vec{\sigma}_1 \times \vec{q}\, \chi_f''(123) \cdot (1 + T_{12}) \chi_f''^{\dagger}(123) \vec{\sigma}_3 \times \vec{q}\, \chi_i'(312)\,, \qquad \text{(B1)}$$

where T_{12} is the two-particle permutation operator and we take particle 3 to be the unlike nucleon. The initial state must be antisymmetric in the pair 1-2 and have spin $\frac{1}{2}$. The final state can be either spin $\frac{1}{2}$ or $\frac{3}{2}$, but it cannot have the unlike spectator pair coupled to spin 0. Therefore, when we sum over the final spins and average over the initial spins, we must utilize the spin projection operators, $P_s^S(i, jk)$, in order to remove the spin functions by use of completeness [$P_0^{1/2}(1, 23)$ projects total spin-$\frac{1}{2}$ states with particles 2-3 coupled to spin 0]. So from Eq. (B1), we have for the spin part

$$\mathcal{S} \equiv \tfrac{1}{2} \sum_i \sum_f (1 + T_{12}) \chi_i'^{\dagger}(312) \vec{\sigma}_1 \times \vec{q}\, \chi_f''(123) \cdot (1 + T_{12}) \chi_f''^{\dagger}(123) \vec{\sigma}_3 \times \vec{q}\, \chi_i'(312)\,, \qquad \text{(B2)}$$

$$= \tfrac{1}{2} \times 4 \sum_{\substack{\text{all possible} \\ \text{spin fcns}}} \sum \chi_i'^{\dagger}(312) \vec{\sigma}_1 \times \vec{q}\,[1 - P_0^{1/2}(1, 23)]\, \chi_f''(123) \cdot \chi_f''^{\dagger}(123) \vec{\sigma}_3 \times \vec{q}\, P_0^{1/2}(3, 12)\, \chi_i'(312)\,, \qquad \text{(B3)}$$

$$= 2\mathcal{T}\{\vec{\sigma}_1 \times \vec{q}\,[1 - P_0^{1/2}(1, 23)] \cdot \vec{\sigma}_3 \times \vec{q}\, P_0^{1/2}(3, 12)\}\,. \qquad \text{(B4)}$$

To obtain Eq. (B4), we have used the completeness relation $\sum \chi\chi^{\dagger} = I_1 I_2 I_3 \equiv 1$ for three particles. I_j is the unit operator in spin space for nucleon j. The trace $\mathcal{T}$ means $\mathrm{Tr}_1 \mathrm{Tr}_2 \mathrm{Tr}_3$. The remainder of the computation is simply trace algebra with Pauli spin matrices. The result is

$$\mathcal{S} = -\vec{q}^{\,2}\,. \qquad \text{(B5)}$$

APPENDIX C. POLE DOMINANCE

The objectives of this Appendix are to demonstrate the relationship of the Griffy-Oakes pole model to wave-function calculations and to justify keeping only the I_1 contributions to the cross sections in the quasielastic region. This is accomplished by studying the coincidence cross sections derived from asymtotic wave functions.[23] The philosophy is that the amplitudes should be determined by the asymptotic structure of the wave functions; at least, apart from normalization. We expect this to be a good approximation, because the electron interacts only (essentially) with the ejected nucleon, leaving the spectator pair either bound or with low relative energy.

The integrals appearing in the cross-section expressions, Eqs. (17)–(20), can now be easily evaluated with the asymptotic wave functions given in Knight, O'Connell, and Prats.[23] We obtain for the two-body breakup

$$I_1(l_i) = N\left(\frac{8\pi\gamma}{1-\gamma r_0}\right)^{1/2} \frac{(4\alpha\beta)^{1/2}}{(\gamma+\alpha)(\beta^2+l_i^2)}, \tag{C1}$$

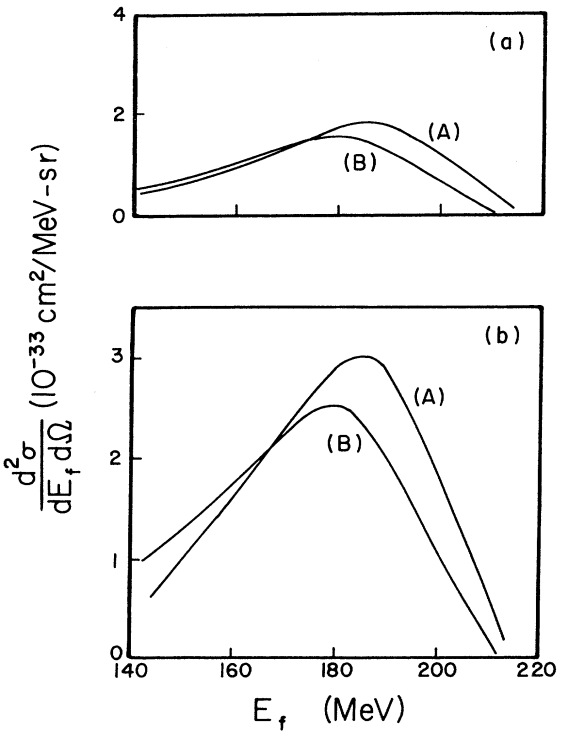

FIG. 11. Comparison of the three-body contribution to the inelastic cross sections, $E_i = 248.8$ MeV and $\theta = 90°$, with and without final-state interactions. Figures (a) and (b) give the results for ^{3}He and ^{3}H, respectively. Curves (A) are results with final-state rescattering between the spectator pair and curves (B) without. Tabakin's parameters are used in all cases.

$$I_2(l_i, l_f) = N\left(\frac{8\pi\gamma}{1-\gamma r_0}\right)^{1/2} \frac{2(4\alpha\beta)^{1/2}}{q(\beta^2+l_f^2)} \tan^{-1}\frac{q}{2(\gamma+\alpha)}, \tag{C2}$$

where the notation is the same as Ref. 23. [Note that the β appearing here is not the same as the one appearing in Eq. (29), etc.] The three-body-breakup results are

$$I_1(l_i, k) = \frac{4\pi N(4\alpha\beta)^{1/2}}{\beta^2+l_i^2}\left(\frac{1}{\alpha^2+k^2}+\frac{f_s(k)}{\alpha-ik}\right), \tag{C3}$$

$$I_2(l_i, l_f, k) = \frac{4\pi N(4\alpha\beta)^{1/2}}{\beta^2+l_f^2}\left(\frac{1}{\alpha^2+(\vec{k}+\frac{1}{2}\vec{q})^2} + \frac{2f_s(k)}{q}\tan^{-1}\frac{q}{2(\alpha-ik)}\right), \tag{C4}$$

where $f_s(k) = (k\cot\delta - ik)^{-1}$ is the two-body scattering amplitude. The $\vec{J}_1$ and $\vec{J}_2$ integrals are essentially the I_1 and I_2 integrals, so we do not display them here.

The fact that the I_2 contribution is negligible in quasielastic scattering can be seen by comparing I_1 and I_2. The ratio written as an inequality is

$$\frac{I_2}{I_1} < \frac{\beta^2+l_i^2}{\beta^2+l_f^2}, \tag{C5}$$

where the right-hand side is bounded by 0.18 for the proton angles 30–60° in the coincidence experiment. For a great part of this range, the ratio is less than 0.10. Moreover, when the two-body coincidence cross section is computed with these wave functions, we find the difference between including the I_2 contribution and neglecting it to be less than 1% at the peak, $\theta_p \sim 52.5°$, and less than 5% at the worst point, $\theta_p = 30.0°$. This is what we would expect from the square of Eq. (C5), and it agrees with the conclusion of Gibson and West[6] for other assumed analytic forms of the wave func-

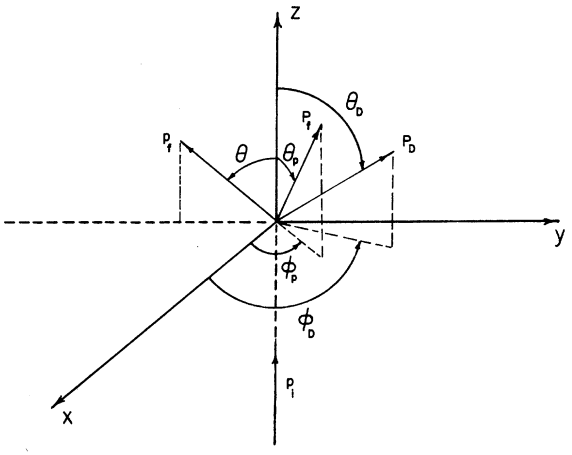

FIG. 12. Kinematics for electrodisintegration.

tions. Analogous study of the three-body breakup leads to similar conclusions. However, outside the range of the coincidence data the I_2 contributions become more important, but we do not include them in the inelastic calculations where we integrate over proton angles. The reason for this comes from the fact that I_2 only becomes important compared with I_1 when l_i increases at the expense of l_f. When this occurs the coincidence cross section decreases rapidly, since it is proportional to l_f. Therefore, the contributions to the inelastic cross section in this region are small, and neglecting the I_2 contributions introduces only small errors. We emphasize that this is valid only in the quasielastic region. For low-energy electron scattering the I_2 contributions are as important as the I_1 contributions throughout.

When the I_2 integrals are neglected, we can compare the asymptotic-wave-function model to the dispersion-theory pole model of Griffy and Oakes.[6] Comparing their cross-section expressions with those derived in Sec. III, we have

$$I_1(P_i)=\frac{\gamma_A}{(\hbar q-P_f)^2-M^2c^2}\approx\frac{\gamma_A}{\frac{3}{2}P_i^{\,2}+2B_2M} \tag{C6}$$

and

$$I_1(P_i,k=0)=\frac{\gamma_{B\text{ or }C}}{(\hbar q-P_f)^2-M^2c^2}\approx\frac{\gamma_{B\text{ or }C}}{\frac{3}{2}P_i^{\,2}+2B_3M}. \tag{C7}$$

γ_A, γ_B, and γ_C are undetermined constants representing the nuclear vertex [see Fig. 1(c)(1)]. Comparison of Eqs. (C1) and (C6) yields $B_2=3\hbar^2\beta^2/4M$ (in agreement with a different determination of β by Knight, O'Connell, and Prats[23]) and

$$\frac{2\gamma_A}{3\hbar^2}=N\left(\frac{8\pi\gamma}{1-\gamma r_0}\right)^{1/2}\frac{(4\alpha\beta)^{1/2}}{(\gamma+\alpha)}. \tag{C8}$$

A similar comparison can be made for reactions (B) and (C), provided it is done with $l_i=0$. Otherwise, we arrive at the contradictory conclusion that $B_3=B_2=3\hbar^2\beta^2/4M$.

The relationships of the pole-model and the asymptotic-wave-function approach, combined with the fact mentioned earlier that the pole model reproduces the shape of the coincidence data, lead to two conclusions. The first is that the pole approximation is valid in the realm where the major contribution to the amplitude comes from the external region in which there is no nuclear interaction between the particles. This is equivalent to saying the kinetic energy is much larger than the interaction energy. Secondly, the asymptotic behavior of the ground-state wave function, which is determined by the relative binding of the three nucleons, governs the shape of the cross section. Of course, the correct magnitude requires a careful treatment of both the initial and final states.

---

†Based on parts of a dissertation submitted to the George Washington University in partial fulfillment of the degree Doctor of Philosophy, 1970.

*National Research Council Postdoctoral Research Associate.

[1]For the references up to mid 1969, see the following review articles: R. D. Amado, Ann. Rev. Nucl. Sci. 19, 61 (1969); L. M. Delves and A. C. Phillips, Rev. Mod. Phys. 41, 497 (1969); A. N. Mitra, in *Advances in Nuclear Physics*, edited by M. Baranger and E. Vogt (Plenum Press, Inc., New York, 1969), Vol. III, p. 1.

[2]J. A. Tjon, B. F. Gibson, and J. S. O'Connell, Phys. Rev. Letters 25, 540 (1970); J. S. McCarthy, I. Sick, R. Whitney, and M. R. Yearian, *ibid.* 25, 884 (1970).

[3]R. F. Frosch, H. L. Crannell, J. S. McCarthy, R. E. Rand, R. S. Safrata, L. R. Suelzle, and M. R. Yearian, Phys. Letters 24B, 54 (1967); B. T. Chertok, E. C. Jones, W. L. Bendel, and L. W. Fagg, Phys. Rev. Letters 23, 34 (1969).

[4]A. Johansson, Phys. Rev. 136, B1030 (1964); C. D. Buchanan *et al.*, in *Proceedings of the International Symposium on Electron and Photon Interactions at High Energies, Hamburg, 1965* (Springer-Verlag, Berlin, Germany, 1965), Vol. I, p. 20; E. B. Hughes, M. R. Yearian, and R. Hofstadter, Phys. Rev. 151, 841 (1966).

[5]Hereafter, we shall mean by inelastic cross-section detection of only the scattered electron, as opposed to coincidence cross section, where both the scattered electron and fast proton are detected.

[6]R. M. Haybron, Phys. Rev. 130, 2080 (1963); T. A. Griffy and R. J. Oakes, *ibid.* 135, B1161 (1964); Rev. Mod. Phys. 37, 402 (1965); B. F. Gibson and G. B. West, Nucl. Phys. B1, 349 (1967); F. C. Khanna, *ibid.* A97, 417 (1967); B. F. Gibson, *ibid.* B2, 501 (1967).

[7]In addition to the above-mentioned theoretical work, there are three other papers in Ref. 6. Haybron's paper concerns the inelastic cross sections and predates the experiments. Khanna's and Gibson's articles are concerned with short-range effects in the ^{3}He ground state, and reaction (A) is used for experimental comparison. In these cases, as well as those mentioned in the text, one or more parameters are determined from three-body data.

[8]Some preliminary results of this work have appeared in D. R. Lehman, Phys. Rev. Letters 23, 1339 (1969).

[9]K. W. McVoy and L. Van Hove, Phys. Rev. 125, 1034 (1962).

[10]This procedure is not strictly valid, since proper definition of relativistic center-of-mass and internal dynamical variables for a weakly bound system introduces M^{-2} corrections to nonrelativistic dynamical calculations. F. E. Close and L. A. Copley, Nucl. Phys. B19, 477 (1970); R. A. Krajcik and L. L. Foldy, Phys. Rev. Letters 24, 545 (1970).

[11]E. B. Hughes, T. A. Griffy, M. R. Yearian, and R. Hofstadter, Phys. Rev. 139, B458 (1965).
[12]T. Janssens, R. Hofstadter, E. B. Hughes, and M. R. Yearian, Phys. Rev. 142, 922 (1966).
[13]I. M. Barbour and A. C. Phillips, Phys. Rev. Letters 19, 1388 (1967); Phys. Rev. C 1, 165 (1970).
[14]This is not the case when I_2 and $\tilde{J}_2$ contributions are included.
[15]Y. Yamaguchi, Phys. Rev. 95, 1628 (1954).
[16]We have not considered the question of gauge invariance for a nonlocal potential. Based on the work of A. M. Korolev, Yadern. Fiz. 6, 353 (1967) [transl.: Soviet J. Nucl. Phys. 6, 257 (1968)], we would expect the magnetic terms of the interaction to be altered.
[17]J. S. O'Connell and F. Prats, Phys. Letters 26B, 197 (1968).
[18]A. G. Sitenko and V. F. Kharchenko, Nucl. Phys. 49, 15 (1963).
[19]F. Tabakin, Phys. Rev. 137, B75 (1965).
[20]H. Collard, R. Hofstadter, E. B. Hughes, A. Johansson, M. R. Yearian, R. B. Day, and R. T. Wagner, Phys. Rev. 138, B57 (1965).
[21]We call the reader's attention to a misprint in the Hughes *et al.* paper. The ordinate in both plots of the ^{3}He data is mislabeled. The ordinate scale should be twice that shown. We would like to thank Dr. E. B. Hughes for verifying this misprint.
[22]These data have not been adjusted for radiative effects. Based on a paper by N. T. Meister and T. A. Griffy, Phys. Rev. 133, B1032 (1964), wherein they develop a simplified method for calculating radiative corrections to the inelastic spectrum, we can qualitatively estimate the correction. They illustrate their method for electron-deuteron scattering at 475-MeV incident energy using Durand's model, L. Durand, III, Phys. Rev. 123, 1393 (1961). The major change in the theoretical curve occurs at the peak where the reduction is less than 10%. The theoretical cross section is reduced for final electron energies below the elastic peak to about midway down the high-energy-transfer side of the quasielastic peak, where the radiative corrections tend to increase the curve. Therefore, we would expect slightly poorer agreement in the low excitation energy part of the spectrum and somewhat improved agreement on the high-energy side of the quasielastic peak, if adjustment for radiative effects were made.
[23]J. M. Knight, J. S. O'Connell, and F. Prats, Phys. Rev. 164, 1354 (1967).

PHYSICAL REVIEW C VOLUME 3, NUMBER 5 MAY 1971

Cluster-Model Vertex Functions for ^{16}O: Backward α-Particle Scattering

J. V. Noble and H. T. Coelho
Physics Department, University of Pennsylvania, Philadelphia, Pennsylvania 19104
(Received 10 November 1970)

We show by direct calculation that the heavy-particle-transfer model of backward elastic α-particle scattering, together with the assumption of α-cluster structure of ^{16}O and ^{12}C, is capable of explaining the large backward peak in elastic α scattering from ^{16}O.

I. INTRODUCTION

Several authors have reported a strong backward peak in the angular distribution of α particles elastically scattered by ^{16}O, at several incident energies.[1-4] Since this backward peak cannot be fitted by the standard optical model (at least, not without considerable adjustment of its parameters) a variety of alternative theoretical descriptions have been proposed including giant resonances,[3] Regge poles,[3] and heavy-particle transfer.[5]

The aim of this paper is to demonstrate that the observed backward peaking is well described by the simplest heavy-particle-transfer (HPT) mechanism, and that the failure of previous authors[1] to reach this conclusion probably results from their approximations. Although we have not yet investigated the other ($4n$) target nuclei (which also exhibit a strong backward peak in elastic α-particle scattering) we feel certain that these data also can be similarly interpreted.

We next describe our formalism; in Sec. III we present the results of our calculations, and in Sec. IV, we enumerate our conclusions and discuss briefly how and why they differ from previous work.

II. THEORY

The extreme backward scattering of α particles involves rather large momentum transfer which may be imparted either by a succession of small impulses or by a fundamentally backward-peaked mechanism such as heavy-particle exchange. In the presence of many open inelastic channels, the consequent absorption of the projectile greatly favors the latter type of process, since the flux loss at each stage of multiple scattering is prohibitive. (This is why it is impossible to fit the backward-scattering data using an optical potential